



## Numerical Analysis of Settlement of a Piled Raft Foundation on Coastal Soil

Syed Raghbir Abbas Shah<sup>1\*</sup>, Aneel Kumar<sup>1</sup>, Muhammad Auchar Zardari<sup>2</sup>,  
Tauha Hussain Ali<sup>2</sup>, Riaz Bhanbhro<sup>2</sup>

<sup>1</sup> Department of Civil Engineering, Mehran University of Engineering and Technology, Jamshoro, Sindh, Pakistan.

<sup>2</sup> Department of Civil Engineering, Quaid-e-Awam University, Nawabshah, Pakistan.

Received 29 September 2022; Revised 06 January 2023; Accepted 18 January 2023; Published 01 February 2023

### Abstract

There is a growing demand for multi-story buildings for residence and commercial purposes in coastal areas of Sindh, Pakistan. Such types of soils are generally considered more compressible with high groundwater levels, which may cause lower shear strength and higher settlement. The computation of the settlement of foundations requires the use of advanced constitutive models, which are not commonly used due to a lack of field or experimental data. This study is carried out to illustrate the use of an advanced soil model, i.e., Hardening Soil Model for the computation of settlement. For this purpose, numerical modeling was carried out using Finite Element Program PLAXIS 2D. Initially, the MC Model was utilized for the calculation of the settlement of a 10-story building in the coastal soil. In addition, parametric analyses for the effects of modulus of elasticity, permeability, and dilatancy angle were carried out. The results mainly suggest that the settlement of the building constructed on a piled raft foundation, predicted with the MC model, was 40% higher than that of the HS model. For prediction of settlement of the piled raft foundation, the results suggest that the HS model can be given preference as compared to the MC model.

**Keywords:** Settlement; Consolidation; Standard Penetration Test; Dilatancy Angle; Permeability.

### 1. Introduction

Due to population growth and urbanization, people from remote areas are migrating towards cities. The coastal areas of Sindh, such as Thatta and Badin, are now becoming familiar among visitors and tourists. For example, Gharo City, located in District Thatta Sindh, Pakistan, is famous for the Sunway Lagoon Water Park. Many of the families, tourists, and visitors come from different cities to enjoy Gharo Sunway Lagoon Water Park. In addition, in the coastal belt of Sindh, particularly in Thatta and Badin districts, there is a likelihood of the construction of wind farms. This indicates that future demand for residential buildings and shopping centers in such regions will be high. The soils of the coastal area of Sindh consist of clay, silt, and sand left by the flowing floodwater of the Indus River. This soil type is primarily less permeable. Generally, the water level is at a very shallow depth. Due to the low permeability of the soils in this region, water logging and soil salinity have emerged as the main problems [1]. In order to ensure the stability and safety of buildings constructed on such coastal soils, it is necessary to investigate the soils up to a sufficient depth in order to know how such soils behave under the sustained load of a multi-story building.

\* Corresponding author: ali.abbas.shah182@gmail.com

 <http://dx.doi.org/10.28991/CEJ-2023-09-02-05>



© 2023 by the authors. Licensee C.E.J., Tehran, Iran. This article is an open access article distributed under the terms and conditions of the Creative Commons Attribution (CC-BY) license (<http://creativecommons.org/licenses/by/4.0/>).

Therefore, for the safe, economical, and sustainable design of the foundations of multi-story buildings, a detailed understanding of the behavior of coastal soils under loading conditions is required to prevent excessive settlement and deformation and the associated structural damage to buildings. To the best of the authors' knowledge, this information is lacking to a great extent. Although several studies have been presented on the numerical analysis of piled raft foundations on clay and sand [2–5], there is no mention of such numerical studies on coastal soils.

In the numerical analysis of settlement, the choice of an appropriate constitutive model plays a key role [6–8]. There are several constitutive models implemented in commercial finite element programs. Generally, it is considered that advanced soil constitutive models such as the Hardening Soil Model perform better in predicting settlement of foundations as compared to the Mohr Coulomb Model [9–12]. It is a challenging task to utilize advanced constitutive models because they require more input parameters. It has been attempted in this paper to demonstrate how an advanced constitutive model can be used for numerical computations when some of its parameters are indirectly evaluated from field tests such as Standard Penetration Tests. In the field of geotechnical engineering, empirical relations may be used to determine soil parameters. However, correlations are not generally reliable. Special caution should be exercised in areas where no prior experience has been gained. This uncertainty must be considered when assessing the reliability of a particular foundation design.

With the availability of powerful computers these days, it may be possible to utilize advanced constitutive models for numerical analysis of various geotechnical problems. The Hardening Soil Model (HSM) is an advanced model for soil response under loading conditions. In HSM, the soil stiffness is described much more accurately by using three different input stiffnesses: the triaxial stiffness  $E_{50}$ , the triaxial unloading stiffness  $E_{ur}$  and the oedometer loading stiffness  $E_{oed}$ . In contrast to the Mohr-Coulomb model, the Hardening Soil model also accounts for the stress-dependency of stiffness moduli. This means that all stiffness increases with pressure. Hence, all three input stiffnesses relate to a reference stress, usually taken as 100 kPa [13]. The piled-raft foundation is considered a 3D case. But, in order to save computational time, such numerical analysis can also be carried out in 2-D space [14–20].

## 2. Materials and Methods

In order to investigate soil properties, eight boreholes were drilled on the coastal soil near Gharo, District Thatta Sindh Pakistan. The soil samples were drilled with rotatory drilling up to a depth of 15 m. Standard Penetration Tests (SPT) were performed on the site to determine  $(N_1)_{60}$  values of the soil. Some basic geotechnical tests were performed on the collected samples. The details of those tests will be presented elsewhere. The depth of excavation was divided into two major portions: (i) silty clay/clayey silt (0–5 m) and (ii) silty fine sand (5–15 m). Numerical calculations of the settlement of a multi-story building on the coastal soil were performed with PLAXIS 2D [13], which is a finite element method-based program for the calculation of various types of geotechnical structures.

The PLAXIS program allows various constitutive models to represent the behavior of geomaterials. Initially, an elastic-plastic Mohr Coulomb (MC) Model [13] was selected for evaluation of settlement of the coastal soil. The MC Model is used for various geotechnical problems because it requires very few input parameters that can be determined through laboratory tests. The following input parameters are needed for the MC model: friction angle, cohesion, permeability, modulus of elasticity, dilatancy angle, and saturated and unsaturated unit weight of the soils. The value of the friction angle of the soils at various depths is presented in Table 1. It can be observed that the minimum value of friction angle for silty clay/clayey silt is  $30^\circ$  and the maximum value is  $43^\circ$ . The minimum value of silty fine sand is  $31^\circ$  and the maximum value is  $44^\circ$ . The range of minimum and maximum values of friction angle for both types of layers indicate the degree of compactness of soils. The range of values of the internal friction angle is in accordance with the findings of the available literature; see, e.g., Das [21], who mentioned friction angle values of dense sand in the range of  $34$  to  $48^\circ$ . The average values of friction angle for silty clay/clayey silt, and silty fine sand are  $34^\circ$  and  $35^\circ$ , respectively. From the laboratory tests on the soil, the value of the cohesion of silty clay/clayey silt was negligible. But, for numerical analysis with PLAXIS, it is recommended to use minimum value of 1 kPa as cohesion for smooth running of calculations. Clays exhibit a low dilation angle. The dilation angle of sand depends on the angle of internal friction. For non-cohesive soils with the angle of internal friction  $\varphi > 30^\circ$ , the value of dilation angle can be estimated as  $\psi = \varphi - 30^\circ$  [22]. The  $(N_1)_{60}$  values of the soil layers at various depths are illustrated in Table 2. The average values of SPT blow counts for silty clay/clayey silt (0–5 m depth) were found to be 14. The average values of SPT blow counts for silty fine sand (5–15 m depth) were found to be 22.

**Table 1. Estimation of friction angle from borehole data**

Soil type	Depth (m)	BH1	BH2	BH3	BH4	BH5	BH6	BH7	BH8	Average
Silty clay/Claey silt	0-5	30 33	34 33	35 32	32		33 41	35 41	37 43	32

<b>Average</b>		31.5	33.5	33.5	32	35.3	38	40	34
		32	35	35	31	34	35	35	40
		34	38	34	38	35	42	38	32
		37	30	37	39	33	37	33	35
Silty fine sand	6-15	33	34	36	36	30	33	34	33
		33	34	33	36	38	34	40	35
		34	35	37	39	35	40	33	44
		36		37		37	35	32	33
<b>Average</b>		34.1	34.3	35.5	36.5	34.5	36.5	35	36

**Table 2. Estimation of average blow count from Standard Penetration Test**

<b>Soil type</b>	<b>Depth (m)</b>	<b>BH1</b>	<b>BH2</b>	<b>BH3</b>	<b>BH4</b>	<b>BH5</b>	<b>BH6</b>	<b>BH7</b>	<b>BH8</b>	<b>Average</b>
Silty clay/ Caley silt	0-5	12	6	13	14	10	10	8	11	
		10	16	16	6	5	29	12	9	
		7	12	11	26	9	10	38	19	14
										38
<b>Average</b>		10.75	11.3	13.3	15.3	8	16.3	19.3	19.2	
Silty fine sand	5-15	10	18	18	16	17	35	20	19	
		16	22	23	11	16	53	26	10	
		33	8	22	25	14	26	15	16	
		14	18	19	55	22	15	9	19	
		20	24	30	24	32	24	40	19	22
		24	12	28	26	17	42	13	19	
		38	27		26	42	24	20	19	
<b>Average</b>		22.1	18.4	23.3	26.1	22.8	31.2	20.4	17.2	

The value of modulus of elasticity of the coastal soils was not directly measured from laboratory tests. The value of the modulus of elasticity of the soils (Table 3) was calculated from suitable correlations [23-26]. The average value of modulus of elasticity for silty clay/clayey silt and silty fine sand was 6340 kPa, and 17660 kPa, respectively. The minimum values of modulus of elasticity of both layers are 5362 kPa and 14740 kPa, respectively. The coefficient of permeability for silty clay/clayey silt was  $1 \times 10^{-10}$  m/s. The coefficient of permeability for silty fine sand was from  $1 \times 10^{-5}$  to  $1 \times 10^{-7}$  m/s [27-33].

**Table 3. Estimation of values of Modulus of Elasticity from SPT blow counts**

<b>Type of soil</b>	<b>Average SPT value</b>	<b>Correlation</b>	<b>Modulus of Elasticity (kN/m<sup>2</sup>)</b>	<b>Reference</b>
Silty clay/clayey silt	14	400(N1) <sub>60</sub>	5600	AASHTO 2002 [23]
		300(N+6)	6000	Bowels 1996 [24]
		E/N = 0.6 to 0.7 MPa	8400	Butler 1975 [25]
		383N	5362	Ruhan Rajapakse 2015 [26]
<b>Average</b>			6340	
Silty fine sand	22	700(N1) <sub>60</sub>	15400	AASHTO 2002 [23]
		500(N+15)	18500	Bowels 1996 [24]
		E/N <sub>60</sub> =1 MPa	22000	Stroud 1989 [25]
		670N	14740	Rajapakse 2015 [26]
<b>Average</b>			17660	

## 2.1. Geometry of the Building Model

As mentioned earlier, the soil profile below the building is mainly divided into two layers. The upper layer (0–5 m) is silty clay/clayey silt. The lower layer (5–15 m) is silty, fine sand. The water level is 1 m below the surface. A 1 m thick raft foundation is used. The width of the raft foundation is 20 m. It is proposed that 10 floors of the building be constructed. The average uniformly distributed load on each floor is taken as 10 kN/m<sup>2</sup> [34–37]. The geometry of the building on the coastal soil is shown in Figure 1. The horizontal boundaries were made sufficiently wide to minimize

the effect of boundaries on the computed results of settlement. The concrete of the raft is modelled with Linear Elastic Model with following properties: Poisson's ratio = 0.15, modulus of elasticity =  $20 \times 10^6$  kN/m<sup>2</sup>, and unsaturated unit weight = 24 kN/m<sup>3</sup>. The finite element mesh of the building is shown in Figure 2. The mesh was sufficiently refined, and it was found that with further refinement of the mesh, there was no significant effect on the computed results. The average element size of the mesh is 0.4 m.

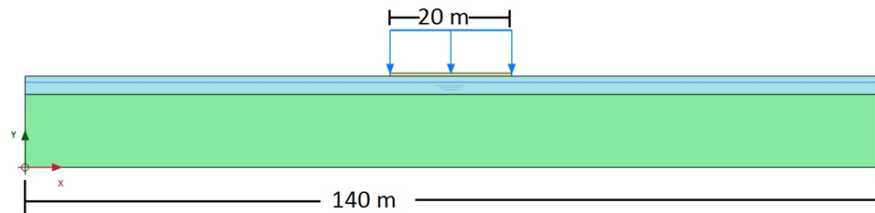


Figure 1. Geometry of the building on coastal soil

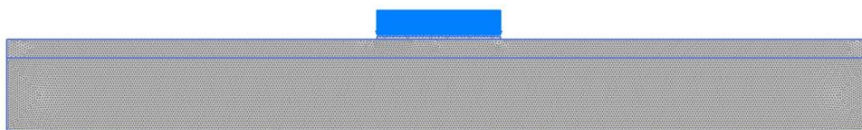


Figure 2. Finite Element mesh of the building

### 3. Results and Discussion

#### 3.1. Calculation of Immediate and Long-Term Settlement of Building

As mentioned earlier, numerical analysis was performed for the immediate and long-term settlement of the building. The building consisted of 10 floors. The uniformly distributed load on each floor was 10 kN/m<sup>2</sup>. According to Skempton and MacDonald [38], the allowable settlement of buildings on raft foundations is as under: Rafts on clay = 65–100 mm, Rafts on sand 50–65 mm. In this case, the soil profile consists of both clay and sand, so 65 mm is taken as the maximum allowable settlement of the building on a raft foundation.

#### 3.2. Case 1.

The average friction angle of the upper layer (silty clay/clayey silt) is taken to be 34°. The average friction angle of the lower layer (silty fine sand) is taken to be 35°. In this case, the dilatancy angle (5°) is not taken into consideration. The average value of modulus of elasticity for silty clay/clayey silt was calculated as 6340 kN/m<sup>2</sup>. The average value of modulus of elasticity for silty fine sand was calculated as 17660 kN/m<sup>2</sup>. The lowest value of modulus of elasticity for silty clay/clayey silt was calculated as 5362 kN/m<sup>2</sup>. The lowest value of modulus of elasticity for silty fine sand was calculated at 14740 kN/m<sup>2</sup>. Settlement of the building was calculated using average modulus of elasticity and lowest modulus of elasticity of both types of layers (Figure 3).

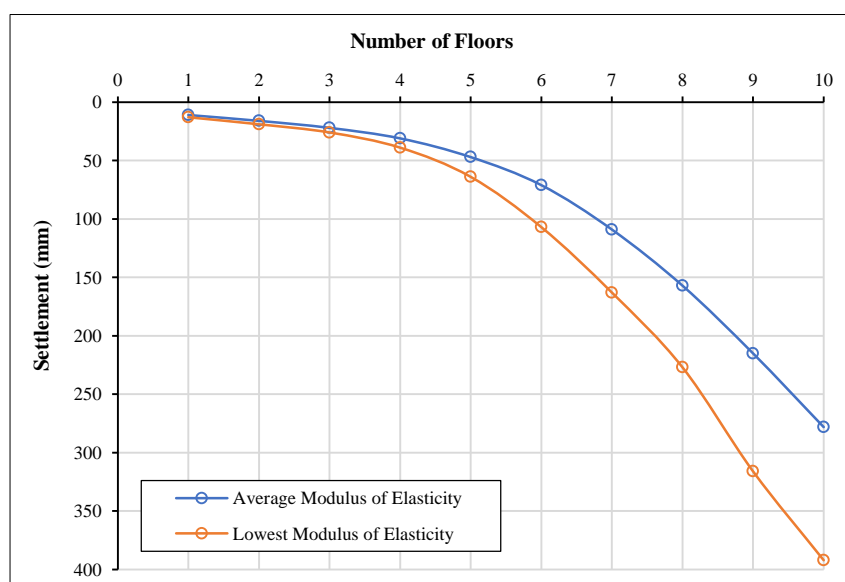
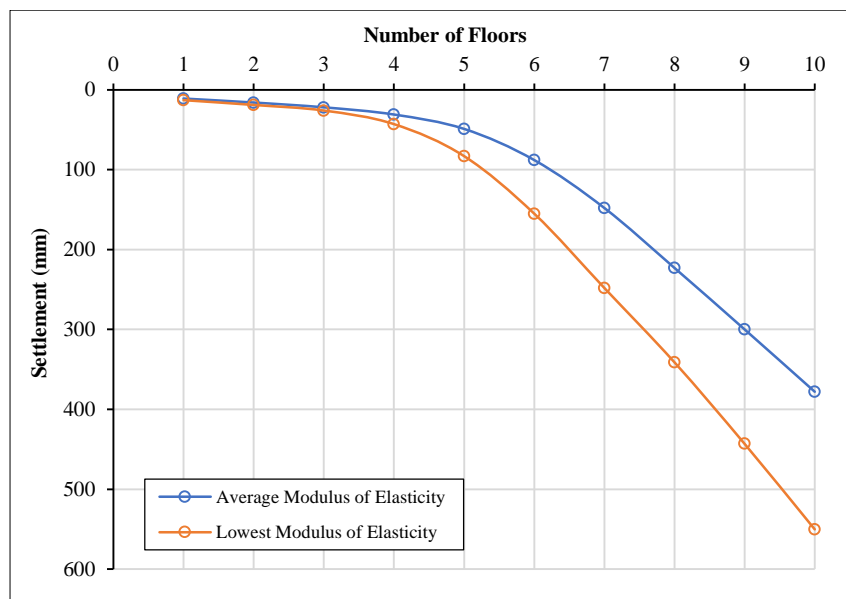


Figure 3. Comparison of settlement calculated using average value of modulus of elasticity and lower value of modulus of elasticity of the two soil layers (case 1)

As the values of average modulus of elasticity of both types of layers are higher than those lower values of modulus of elasticity. Therefore, the magnitude of the settlement is higher in case of lower values of modulus of elasticity. For both average and lower values of modulus of elasticity of the two soil layers, the settlement of the building after construction of 10th floor is greater than the allowable limit. In case of average value of modulus of elasticity, the soil is able to sustain up to 5th floor of the building. In case of lowest value of modulus of elasticity, the soil is also able to sustain up to 5<sup>th</sup> floor of the building. However, at 10<sup>th</sup> floor of the building, the settlement calculated with average modulus of elasticity is about 41% lower than that of calculated with lowest modulus of elasticity.

### 3.3. Case 2

Minimum value of friction angle of  $30^0$  is used for both layers. The other parameters are the same as mentioned in case 1. Comparison of settlement calculated using average and lowest moduli of elasticity is presented in Figure 4. When the value of friction angle of the soil is decreased to  $30^0$  for both the layers, there is increase in settlement. For 10<sup>th</sup> floor, when it is compared with average values of the friction angle (case 1), the settlement calculated with average modulus of elasticity (case 2) is about 36% more than the case 1. For 10<sup>th</sup> floor, when it is compared with lowest values of the friction angle (case 1), the settlement calculated with lowest value of modulus of elasticity (case 2) is about 40% more than the case 1. In case of average value of modulus of elasticity, the soil is able to sustain up to 5<sup>th</sup> floor of the building. In case of lowest value of modulus of elasticity, the soil is able to sustain up to 4<sup>th</sup> floor of the building. The comparison of graphs shown in case 1 and case 2 show that friction angle has also significant effect on settlement of the soil. This implies that as the value of the friction angle decreases, the magnitude of the settlement increases.



**Figure 4. Comparison of settlement calculated using average value of modulus of elasticity and lower value of modulus of elasticity of the two soil layers (case 2)**

### 3.4. Case 3

Effect of dilatancy angle of  $50^0$  of silty fine sand on settlement of the building was evaluated. Remaining parameters are the same as in case 1. Comparison of settlement calculated using average and lowest moduli of elasticity is presented in Figure 5. In case of average value of modulus of elasticity, the soil is able to sustain up to 6<sup>th</sup> floor of the building. In case of lowest value of modulus of elasticity, the soil is able to sustain up to 5<sup>th</sup> floor of the building. In case when dilatancy of silty fine sand is considered, the settlement at 10<sup>th</sup> floor of the building computed with average modulus of elasticity is about 13% less than that of calculated in case 1 (when dilatancy is not included).

### 3.5. Long-Term Settlement

For the above mentioned three cases, the long-term settlement of the building was also calculated for 10, 20, 30, 40, and 100 years. The initial construction of 10 floors of the building takes about 2 years. The settlement after end of the construction and the long-term settlement is shown in the following Figures 6 to 8. It can be observed that the main increment of the long-term settlement of the building occurred during first 10 years after the initial two years of construction. Then in the long term up to 100 years, the magnitude of the settlement remained approximately constant. This is because, the excess pore pressure which increased during construction phase mainly dissipated during initial 10 years after end of construction period. It can be observed that the consolidation process of the soil has been completed relatively in a shorter duration of 10 years, this is because of relatively high permeability of the lower soil layer, i.e., silty fine sand.

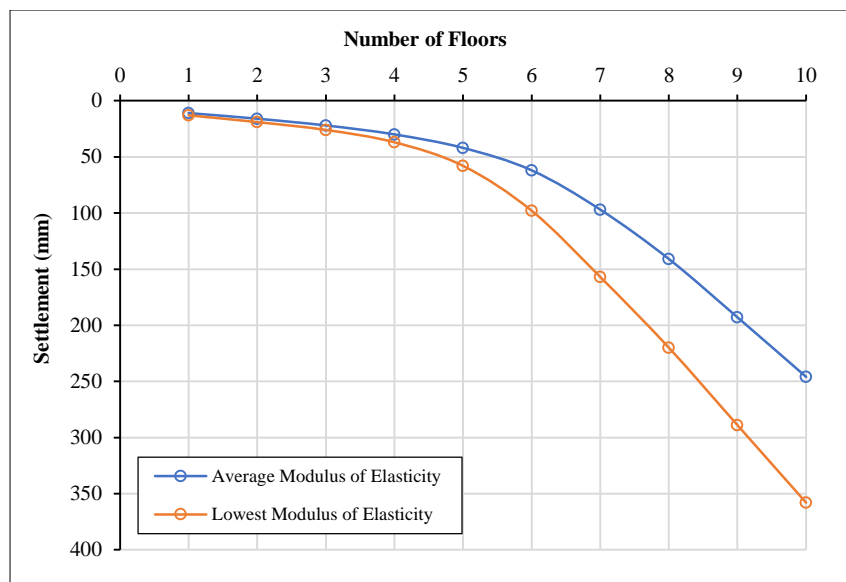


**Figure 5. Comparison of settlement calculated using average value of modulus of elasticity and lower value of modulus of elasticity of the two soil layers (case 1, when dilatancy angle of silty fine sand is taken as 50)**

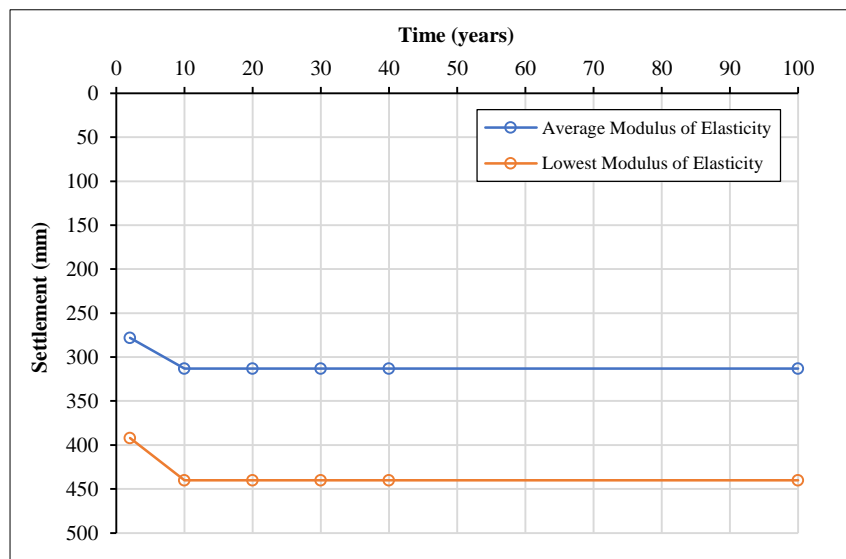


**Figure 6. Comparison of long-term settlement calculated using average and lowest moduli of elasticity (case 1)**

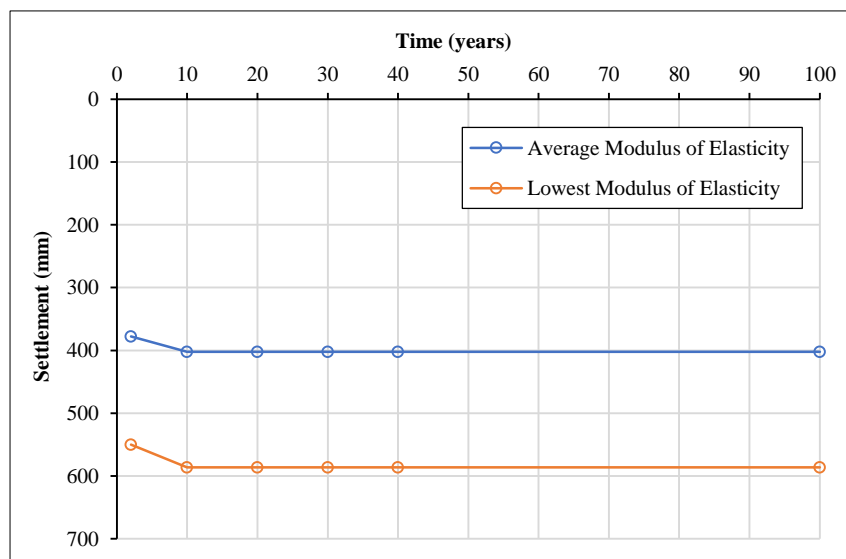


**Figure 7. Comparison of long-term settlement calculated using average and lowest moduli of elasticity (case 2)**

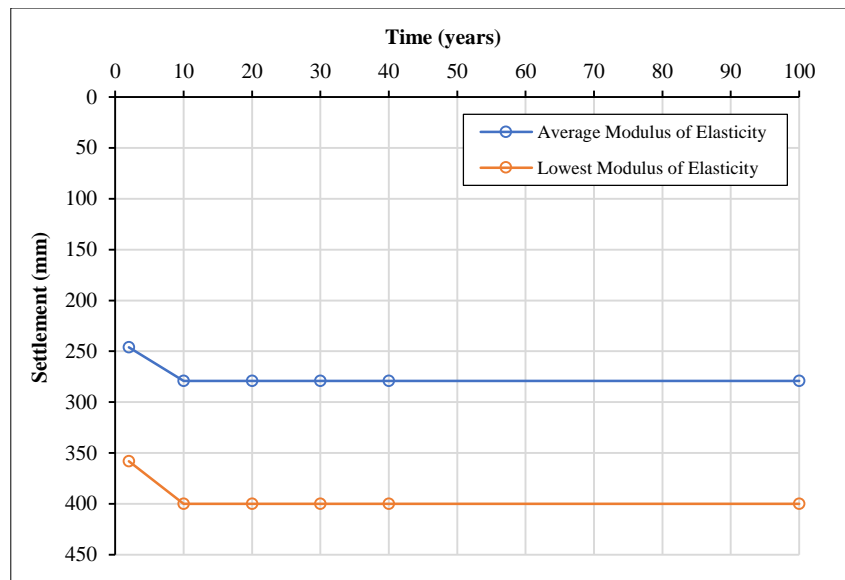


**Figure 8. Comparison of long-term settlement calculated using average and lowest moduli of elasticity (case 3)**

Long term settlement of the building is also evaluated in terms of percentage of the end of construction settlement (Table 4). In case 1 and 3, the long-term settlement is about 13% more than the end of construction settlement. In case 2, the long-term settlement is about 7% more than the end of construction settlement. Comparison of end of construction settlement and long-term settlement for case 1 and case 2 is also presented in Table 5. When the friction angle values of the both the upper and lower soil layers were taken as  $30^\circ$  instead of  $34^\circ$  and  $35^\circ$ , the settlement was more in the case 2 (when friction angle is taken as  $30^\circ$ ) for both the layers. In case of lowest modulus of elasticity, 40% more settlement is calculated for end of construction, and 33% more long term settlement is calculated. Table 6 shows that there is about 41% more settlement for end of construction condition and long-term period.

**Table 4. Long term settlement as a percentage of End of construction settlement**

	Description	End of construction settlement (mm)	Long term settlement (mm)	% increase with end of construction settlement
Case 1	Average modulus of elasticity	278	313	13
	lowest modulus of elasticity	392	440	12
Case 2	Average modulus of elasticity	378	402	6
	lowest modulus of elasticity	550	586	7
Case 3	Average modulus of elasticity	246	279	13
	lowest modulus of elasticity	358	400	12

**Table 5. Effect of values of friction angle (case 1) on settlement of the building (case 2)**

	Description	End of construction settlement (mm)	Long term settlement (mm)	% increase of settlement of case 1 compared with case 2	
				End of construction	Long term
Case 1	Average modulus of elasticity	278	313	36	28
	lowest modulus of elasticity	392	440	-	-
Case 2	Average modulus of elasticity	378	402	-	-
	lowest modulus of elasticity	550	586	40	33

**Table 6. Effect of increase of modulus of elasticity of soils on settlement (comparison between average modulus of elasticity and lowest modulus of elasticity of soils)**

	Description	End of construction settlement (mm)	Long term settlement (mm)	% increase of settlement at end of construction	% increase of settlement at long term
Case 1	Average modulus of elasticity	278	313	41	41
	Lowest modulus of elasticity	392	440		

### 3.6. Effect of Value of Permeability of Lower Layer (Silty Fine Sand) of 5-15 m Depth on Immediate and Long-Term Settlement

As mentioned before, the range of permeability values of silty fine sand is  $10^{-5}$  to  $10^{-7}$  m/s. All the material properties are used as mentioned in case 1. Here the average values of modulus of elasticity of both the layers are used. The average value of modulus of elasticity for silty clay/clayey silt was calculated as  $6340 \text{ kN/m}^2$ . The average value of modulus of elasticity for silty fine sand was calculated as  $17660 \text{ kN/m}^2$ . Referring to Figures 9 and 10, when the average modulus of elasticity is used for both the layers, the higher value of permeability (i.e.,  $10^{-5}$  m/s) showed about 20% less settlement than the case with lower permeability (i.e.,  $10^{-7}$  m/s) for both the end of construction settlement and long-term settlement.

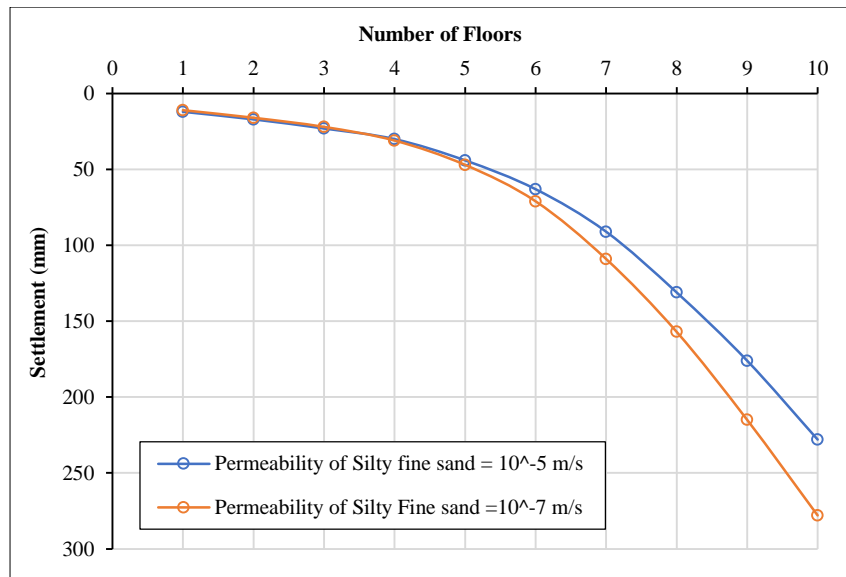


Figure 9. Comparison of end of construction settlement of the building when the permeability of silty fine sand (lower layer) was varied from  $10^{-5}$  to  $10^{-7}$  m/s. In this case average modulus of elasticity of both the layers are used



Figure 10. Comparison of long-term settlement of the building when the permeability of silty fine sand (lower layer) was varied from  $10^{-5}$  to  $10^{-7}$  m/s. In this case average modulus of elasticity of both the layers are used

### 3.7. Lowest Values of Modulus of Elasticity of Both the Layers

All the material properties are used as mentioned in case 1. The lowest value of modulus of elasticity for silty clay/clayey silt was taken as  $5362 \text{ kN/m}^2$ . The lowest value of modulus of elasticity for silty fine sand was taken as  $14740 \text{ kN/m}^2$ . According to Figures 11 and 12, when the lowest values of modulus of elasticity of both the layers are used, in this case, the higher value of permeability (i.e.,  $10^{-5}$  m/s) showed about 16% less settlement than the case with lower permeability (i.e.,  $10^{-7}$  m/s) for both end of construction settlement and long-term settlement.

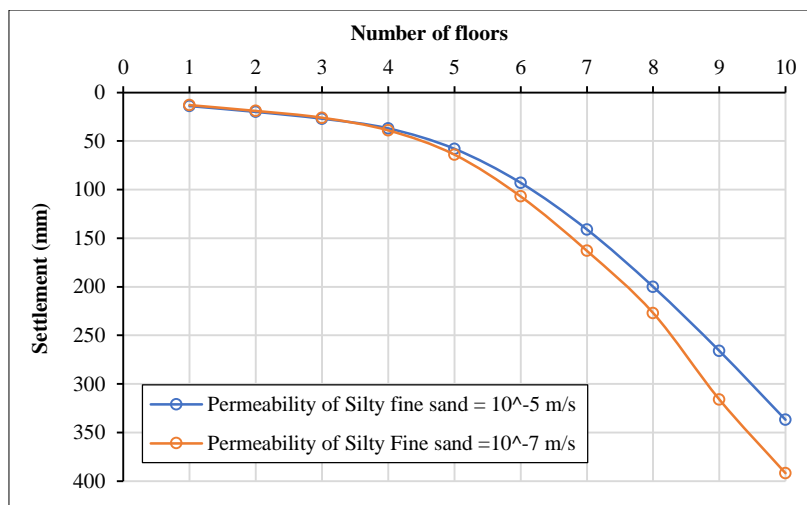


Figure 11. Comparison of end of construction settlement of the building when the permeability of silty fine sand (lower layer) was varied from  $10^{-5}$  to  $10^{-7}$  m/s. In this case lowest modulus of elasticity of both the layers are used



Figure 12. Comparison of long-term settlement of the building when the permeability of silty fine sand (lower layer) was varied from  $10^{-5}$  to  $10^{-7}$  m/s. In this case lowest modulus of elasticity of both the layers are used

### 3.8. Excess Pore Pressure

The excess pore pressures below the phreatic level, where the soil is fully saturated, are denoted with a negative sign, whereas the excess pore pressures above the phreatic level (suction), where the soil is unsaturated, are represented with a positive sign. As can be seen from the Figures 13 to 15, as the loading of each floor is increased on building, there is corresponding increase of excess pore pressure. Say, for instance, that the maximum excess pore pressure after construction of the 1<sup>st</sup> floor, 5<sup>th</sup> floor, and 10<sup>th</sup> floor is respectively, 22, 64, and 110 kN/m<sup>2</sup>. During long-term periods, say for instance 10 and 20 years (Figures 16 and 17), the excess pore pressures are dissipated due to the consolidation process. The magnitude of excess pore pressure was reduced from 110 kN/m<sup>2</sup> (at the end of the construction of the 10<sup>th</sup> floor) to 9 kN/m<sup>2</sup> after 10 years. Further dissipation of excess pore pressure occurred with time. At the end of 20 years, the magnitude of excess pore is greatly reduced to 3.4 kN/m<sup>2</sup>.

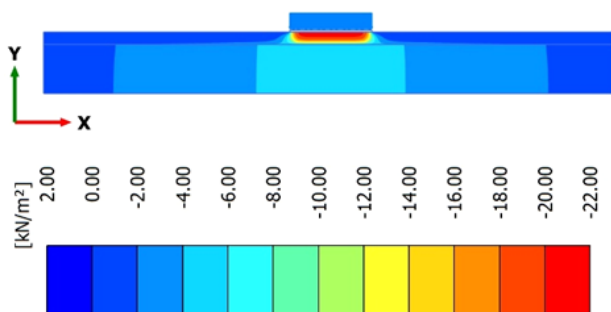
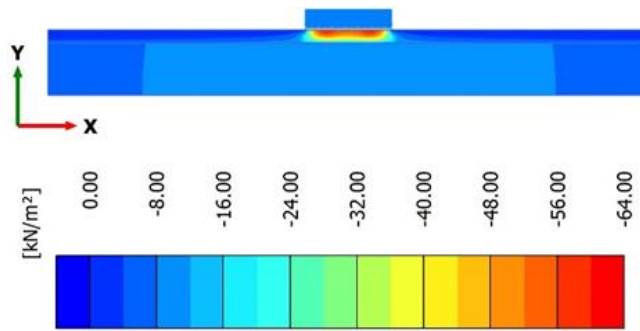
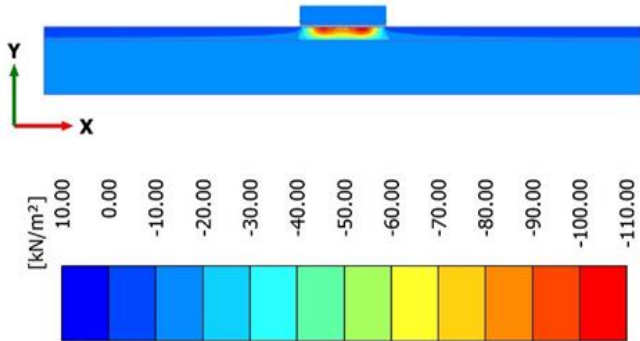


Figure 13. Increase of excess pore pressure at the end of construction of first floor



**Figure 14.** Increase of excess pore pressure at the end of construction of fifth floor



**Figure 15.** Increase of excess pore pressure at the end of construction of tenth floor

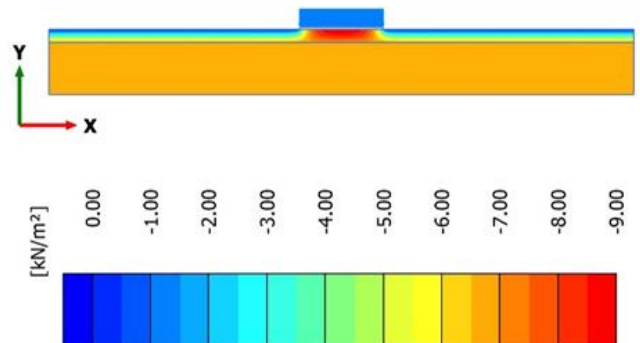


**Figure 16.** Dissipation of excess pore pressure after 10 years from end of construction of tenth floor

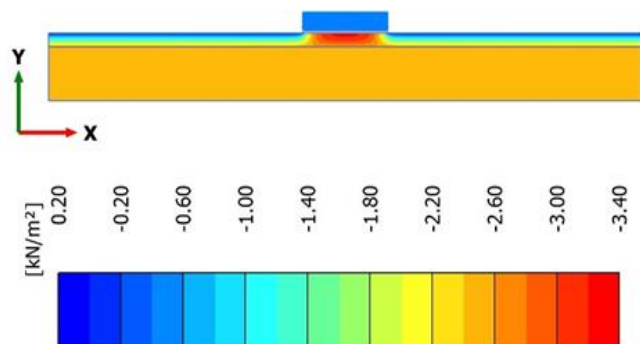


**Figure 17.** Dissipation of excess pore pressure after 20 years from end of construction of tenth floor

### 3.9. Pattern and Distribution of Total Displacement of the Building

It can be observed that the displacement is mainly concentrated below the zone where the load is applied. The main concentration of the displacement is in the zone of silty clay/clayey silt. Then the lower magnitude of the displacement continues to extend below the layer of silty fine sand (Figure 18). From the 5th floor and onward, differential settlement pattern was observed, with more settlement on the edges compared to the central portion (Figures 19 to 21). In the long term, from 10 to 100 years, differential settlement was also observed.

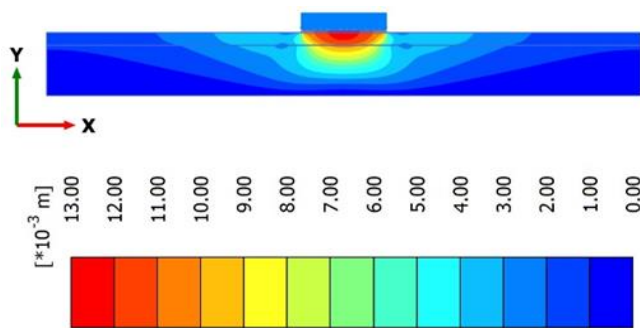


**Figure 18. Displacement pattern of the building after construction of first floor**

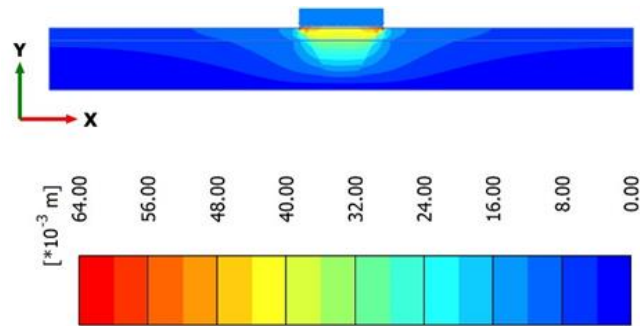


**Figure 19. Displacement pattern of the building after construction of fifth floor**

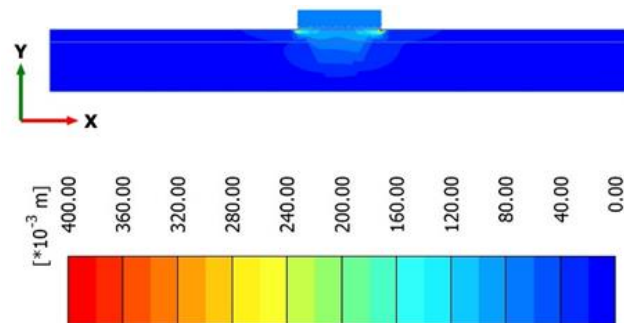


**Figure 20. Displacement pattern of the building after construction of tenth floor**

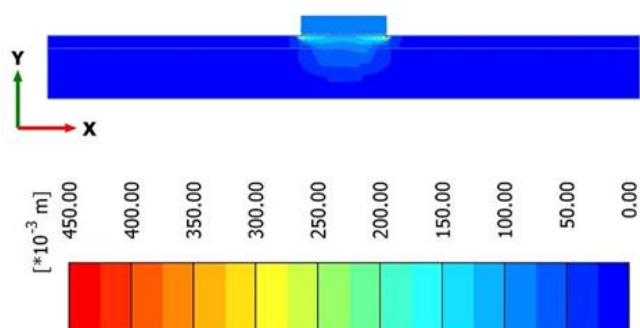


**Figure 21. Displacement pattern of the building after construction of tenth floor and after a period of 10 years**

#### 4. Comparison of Settlement Predicted with MCM and HSM Using Piled Raft Foundation

Initially, preliminary calculations were performed based on a simple MC model. In this case, only 1 m thick raft foundation was used without pile foundation. The main purpose of utilizing the MC Model was to conduct parametric analysis to find out the effect of various parameters on the overall settlement of the building. The calculations indicate that the settlement was beyond the allowable limit of 65 mm after the construction of the 10th story of the building. It was decided to adopt a piled raft foundation. Seventeen circular concrete piles of 0.5 m diameter thickness were equally placed below raft foundation of width 20 m and thickness 1 m as shown in Figure 22. The length of all the piles is 35 m. The piles were modeled with Linear Elastic Model with the following material properties: Young's modulus =  $30 \times 10^6$  kN/m<sup>2</sup>, and Poisson's ratio = 0.1.

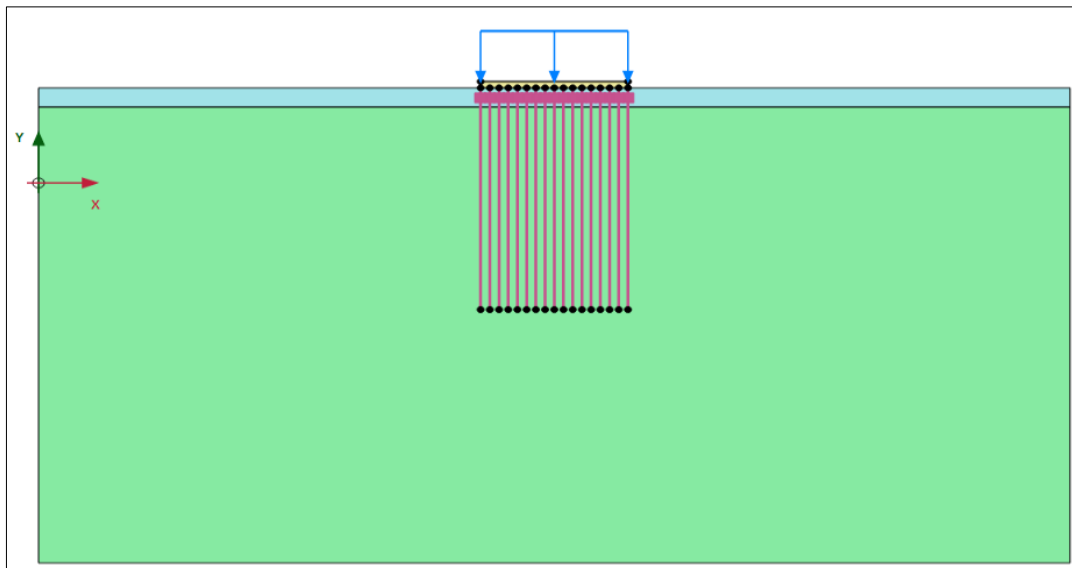


**Figure 22. Piled raft foundation of the multi-story building**

In addition to the MC Model, an advanced elastoplastic model called the Hardening Soil (HS) Model was also utilized for prediction of the settlement. The length and number of piles were increased in order to reduce the settlement to the allowable limit of 65 mm. The additional soil parameters of the HS Model are shown in Table 7. The HS Model gives 40% less settlement as compared to the MC Model during the construction phase, as shown in Figure 23. In the long term phase, the HS Model predicts 35% less settlement as compared to the MC Model predictions as shown in Figure 24.

**Table 7. Additional input parameters of HS Model**

Parameter	Value	Unit	Soil type
Secant stiffness in standard drained triaxial test	6340	kN/m <sup>2</sup>	Silty clay/Claey silt
Tangent stiffness for primary Oedometer loading	6340	kN/m <sup>2</sup>	Silty clay/Claey silt
Unloading/reloading stiffness	19020	kN/m <sup>2</sup>	Silty clay/Claey silt
Secant stiffness in standard drained triaxial test	17660	kN/m <sup>2</sup>	Silty fine sand
Tangent stiffness for primary Oedometer loading	17660	kN/m <sup>2</sup>	Silty fine sand
Unloading/reloading stiffness	52980	kN/m <sup>2</sup>	Silty fine sand

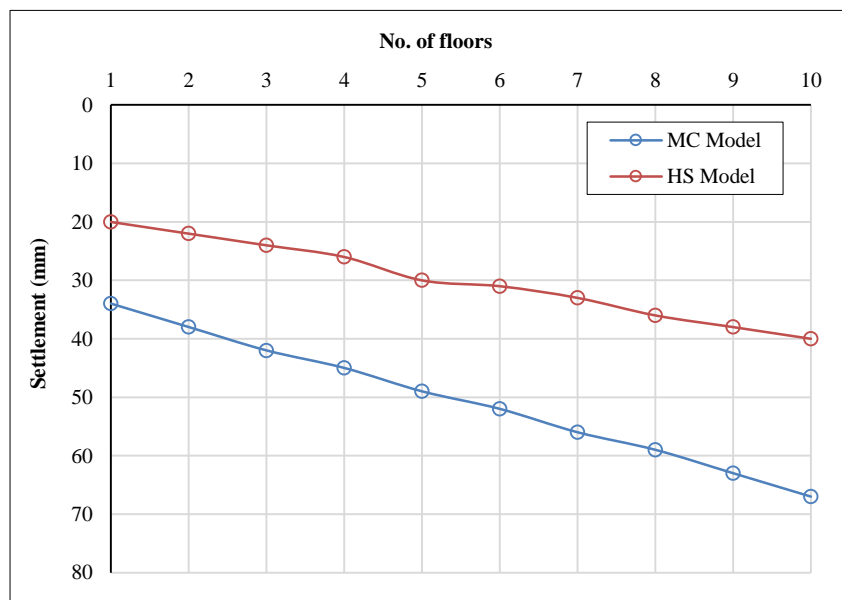


**Figure 23. Comparison of construction settlement of the multi-story building on piled raft foundation up to 10<sup>th</sup> floor using MC Model and HS Model**

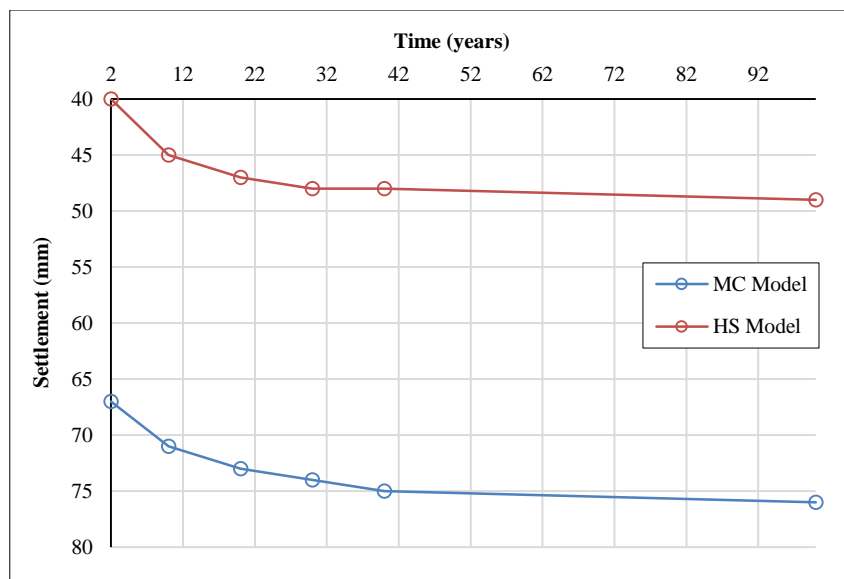


**Figure 24. Comparison of construction settlement of the multi-story building on piled raft foundation across time using MCM and HSM**

## 5. Discussion

It is generally accepted that the most reliable approach for determining the design parameters of subsurface soils is soil sampling in conjunction with laboratory or field tests. In certain instances, different types of relationships might be required to estimate the geotechnical parameters from the values derived from the in-situ and laboratory tests, due to the unavailability of equipment and financial and time constraints in a project. In certain circumstances, however, soil type, water table elevation, and SPT (Standard Penetration Test) blow counts are available to investigate the conditions of the subsurface soil. As mentioned earlier, this study deals with the settlement response of a multi-story building in coastal soil of Sindh, Pakistan. This study is unique in nature because no such study regarding the material properties and response of soil under applied loading conditions is presented in the literature.

Since the calculation of the settlement requires the values of the modulus of elasticity of the soils. In this study, the values of the moduli of elasticity of the soils (i.e., silty clay/clayey silt, and silty fine sand) were obtained using correlations. Therefore, the average values of both soil layers are recommended to be included in the numerical modeling process. In addition, for silty sand layers, the literature suggests permeability values in the range of  $10^{-5}$  to  $10^{-7}$  m/s. As the calculations showed, there was 16% less reduction in the settlement when the lowest values of moduli of elasticity were used. In order to be on the safe side, it is recommended to use a lower value of permeability (i.e.,  $10^{-7}$  m/s) in the numerical modeling. It is also recommended to use the average value of friction angles of  $34^\circ$  and  $35^\circ$  for silty clay/clayey silt, and silty fine sand instead of the lowest value of  $30^\circ$ . By referring to Table 1, it can be noticed that the upper layer (silty clay/clayey silt) and lower layer (silty fine sand) have maximum values of friction angle of  $43^\circ$  and  $44^\circ$  respectively. Even though inclusion of the dilatancy angle shows a 10% reduction in settlement, the dilatancy angle causes unrealistic tensile pore pressure; therefore, it is advised not to include dilatancy in the numerical modeling process.

As mentioned in the paper, the HS Model is an advanced constitutive model that requires more material properties as compared to the simple MC Model. However, the MC Model generally overestimates the rate of settlement of the buildings. For economical and sustainable design of piled raft foundations of multi-story buildings, it is suggested to adopt the HS Model as compared to the MC Model.

## 6. Conclusion

In this study, settlement of a multi-story building constructed on a piled raft foundation on coastal soil was predicted with the MC model and the HS model. The main conclusions drawn from this study are summarized below: The MC model showed 40% more settlement as compared with the HS model. For a safe, sustainable, and economical foundation on coastal soils, it would be best to utilize the HS model for prediction of settlement as compared to the MC model. In addition to the modulus of elasticity of the soils, the reduction of the values of the friction angle has also had a significant effect on the increase in settlement of the building. The effect of including the dilatancy angle of silty fine sand showed about a 10% reduction in settlement as compared with the case without the dilatancy angle. It would be a suitable approach to exclude the dilatancy angle of the silty fine sand in the numerical modeling process. This paper shows that input parameters of the Hardening Soil Model evaluated from the Standard Penetration Test can be utilized for the computation of settlement of piled raft foundations on coastal soils.

## 7. Declarations

### 7.1. Author Contributions

Conceptualization, S.R.A.S., A.K., M.A.Z., and T.H.A.; methodology, S.R.A.S., A.K., and M.A.Z.; software, M.A.Z., and R.B.; validation, S.R.A.S., and R.B.; formal analysis, R.B., and M.A.Z.; investigation, S.R.A.S., and R.B.; resources, A.K.; data curation, S.R.A.S., M.A.Z., and T.H.A.; writing—original draft preparation, S.R.A.S., A.K., M.A.Z., and T.H.A.; writing—review and editing, S.R.A.S., R.B., T.H.A., A.K., and M.A.Z.; visualization, S.R.A.S.; supervision, A.K., and M.A.Z.; project administration, A.K., M.A.Z., T.H.A., and R.B.; funding acquisition, A.K. All authors have read and agreed to the published version of the manuscript.

### 7.2. Data Availability Statement

Data sharing is not applicable to this article.

### 7.3. Funding

The authors received no financial support for the research, authorship, and/or publication of this article.

### 7.4. Acknowledgment

The authors would like to acknowledge Mehran University of Engineering and Technology, Jamshoro and Quaid-e-Awam University, Nawabshah for providing necessary support for conducting this research.

### 7.5. Conflicts of Interest

The authors declare no conflict of interest.

## 8. References

- [1] Majeed, S., Zaman, S. B., Ali, I., & Ahmed, S. (2010). Situational analysis of Sindh coast-issues and options. *Managing Natural Resources for Sustaining Future Agriculture, Research Briefings*, 2(11), 1-23.
- [2] Deb, P., & Pal, S. K. (2022). Structural and geotechnical aspects of piled raft foundation through numerical analysis. *Marine Georesources and Geotechnology*, 40(7), 823–846. doi:10.1080/1064119X.2021.1943083.
- [3] Tian, W., & Galaa, A. (2021). Plate load test on rock with soaking under a massive raft foundation. *Innovative Infrastructure Solutions*, 6(1), 45. doi:10.1007/s41062-020-00434-4.
- [4] Amornfa, K., Quang, H. T., & Tuan, T. V. (2022). 3D numerical analysis of piled raft foundation for Ho Chi Minh City subsoil conditions. *Geomechanics and Engineering*, 29(2), 183–192. doi:10.12989/gae.2022.29.2.183.
- [5] Ferchat, A., Benmebarek, S., & Houhou, M. N. (2021). 3D numerical analysis of piled raft interaction in drained soft clay conditions. *Arabian Journal of Geosciences*, 14(5). doi:10.1007/s12517-021-06783-3.
- [6] Pande, G. N., & Pietruszczak, S. (2021). A critical look at constitutive models for soils. *Geomechanical Modelling in Engineering Practice*, 369–393, Routledge, Abingdon, United Kingdom. doi:10.1201/9780203753583-19.
- [7] Knabe, T., Schweiger, H. F., & Schanz, T. (2012). Calibration of constitutive parameters by inverse analysis for a geotechnical boundary problem. *Canadian Geotechnical Journal*, 49(2), 170–183. doi:10.1139/t11-091.
- [8] Schweiger, H. F., Fabris, C., Ausweiger, G., & Hauser, L. (2019). Examples of successful numerical modelling of complex geotechnical problems. *Innovative Infrastructure Solutions*, 4(1), 1–10. doi:10.1007/s41062-018-0189-5.
- [9] Brinkgreve, R. B. J., & Vermeer, P. A. (1998). Finite element code for soil and rock analyses. AA Balkema, Rotterdam, Netherlands.
- [10] Hsiung, B. C. B., & Dao, S. D. (2014). Evaluation of constitutive soil models for predicting movements caused by a deep excavation in sands. *Electronic Journal of Geotechnical Engineering*, 19(Z5), 17325–17344.
- [11] Phien-Wej, N., Humza, M., & Zaw Aye, Z. (2012). Numerical modeling of diaphragm wall behavior in Bangkok soil using hardening soil model. *Geotechnical Aspects of Underground Construction in Soft Ground*, 715–722. doi:10.1201/b12748-97.
- [12] Teo, P. L., & Wong, K. S. (2012). Application of the Hardening Soil model in deep excavation analysis. *IES Journal Part A: Civil & Structural Engineering*, 5(3), 152–165. doi:10.1080/19373260.2012.696445.
- [13] Brinkgreve, R. B. J., Kumarswamy, S., Swolfs, W. M., Waterman, D., Chesaru, A., & Bonnier, P. G. (2016). PLAXIS 2016. PLAXIS company (Plaxis bv), Netherlands.
- [14] Wulandari, P. S., & Tjandra, D. (2015). Analysis of piled raft foundation on soft soil using PLAXIS 2D. *Procedia Engineering*, 125, 363–367. doi:10.1016/j.proeng.2015.11.083.

- [15] Elwakil, A. Z., & Azzam, W. R. (2016). Experimental and numerical study of piled raft system. *Alexandria Engineering Journal*, 55(1), 547–560. doi:10.1016/j.aej.2015.10.001.
- [16] Ryltenius, A. (2011). FEM modelling of piled raft foundations in two and three dimensions. Master Thesis, Department of Construction Sciences, Geotechnical Engineering, Lund University, Lund, Sweden.
- [17] Balakumar, V., Huang, M., Oh, E., & Balasubramaniam, A. S. (2018). A critical and comparative study on 2D and 3D analyses of raft and piled raft foundations. *Geotechnical Engineering*, 49(1), 150–164.
- [18] Algulin, J. O. E. L., & Pedersen, B. J. Ö. R. N. (2014). Modelling of a piled raft foundation as a plane strain model in PLAXIS 2D. Master Thesis, Department of Civil and Environment Engineering, Division of Geo-Engineering, Chalmers University, Göteborg, Sweden.
- [19] Ukritchon, B., Faustino, J., & Keawsawasvong, S. (2016). A numerical study of load distribution of pile group foundation by 2D model. *Walailak Journal of Science and Technology*, 13(8), 669–688.
- [20] Hong, C. Y., Lee, L. M., Ti, K. S., & Yee, W. S. (2021). A Parametric Study of Piled Raft Foundation in Clay Subjected to Concentrated Loading. *International Journal of Integrated Engineering*, 13(4), 263–274. doi:10.30880/ijie.2021.13.04.025.
- [21] Das, B. M. (2021). Principles of geotechnical engineering. Cengage Learning, Boston, United States.
- [22] Bolton, M. D. (1986). The strength and dilatancy of sands. *Géotechnique*, 36(1), 65–78. doi:10.1680/geot.1986.36.1.65.
- [23] AASHTO. (2002). Standard specifications for highway bridges (17<sup>th</sup> Ed.). American Association of States Highway and transportation Officials, Washington, United States.
- [24] Butler, F. G. (1974). Heavily over-consolidated clays. Proceedings BGS conference on settlement of structures, 531-578, Wiley, London, United Kingdom.
- [25] Stroud, M. A. (1988). The standard penetration test—its application and interpretation. Conference on Penetration Testing, 6-8 July, 1988, London, United Kingdom.
- [26] Rajapakse, R. (2015). *Geotechnical Engineering Calculations and Rules of Thumb*: Second Edition. Butterworth-Heinemann, Oxford, United Kingdom. doi:10.1016/c2015-0-01445-9.
- [27] Wood, D. (2009). *Soil Mechanics: A One-Dimensional Introduction*. Cambridge University Press, Cambridge, United Kingdom. doi:10.1017/CBO9780511815553.
- [28] Ou, C. Y. (2014). Deep excavation: Theory and practice. CRC Press, Boca Raton, United States. doi:10.1201/9781482288469
- [29] Cashman, P. M., & Preene, M. (2020). Groundwater lowering in construction: a practical guide to dewatering. CRC Press, Boca Raton, United States. doi:10.1201/9781003050025.
- [30] Mitchell, J. K., & Soga, K. (2005). *Fundamentals of soil behavior*. John Wiley & Sons, New York, United States.
- [31] Terzaghi, K., Peck, R. B., & Mesri, G. (1996). *Soil mechanics in engineering practice*. John Wiley & Sons, New York, United States.
- [32] Craig, R. F. (2004). *Craig's soil mechanics*. CRC Press, Boca Raton, United States. doi:10.4324/9780203494103.
- [33] Wagner, J. F. (2013). Mechanical properties of clays and clay minerals. *Developments in clay science*. Elsevier, Amsterdam, Netherlands.
- [34] Hageman, J. M. (2008). *Contractor's Guide to the Building Code*. Craftsman Book Company, Carlsbad, United States.
- [35] Ching, F. D., & Winkel, S. R. (2021). *Building Codes Illustrated: A Guide to Understanding the 2021 International Building Code*. John Wiley & Sons, New York, United States.
- [36] Ambrose, J. (1993). *Building structures*. John Wiley & Sons, New York, United States.
- [37] Salvadori, M. (2000). *The Art of Construction: projects and principles for beginning engineers & architects*. Chicago Review Press.
- [38] Skempton, A. W., & Macdonald, D. H. (1956). The Allowable Settlements of Buildings. *Proceedings of the Institution of Civil Engineers*, 5(6), 727–768. doi:10.1680/ipeds.1956.12202.